Numerical Investigation of a Transonic Axial Compressor Stage with Inlet Distortions

Andreas Lesser* and Jens Iseler,†
Reinhard Niehuis ‡
Institut für Strahlantriebe
University of the German Armed Forces Munich, 85577 Neubiberg, Germany

Abstract

The topic of this paper is the numerical modelling of an inlet flow distortion and it's subsequent effect on a transoniccompressor stage. Two codes, specialized for these respective problems, are coupled using a highly reliable method described in the paper. TAU developed by the German Aerospace Center, Institute of Aerodynamics and Flow Technology, is used to model the inlet distortion while TRACE, from the German Aerospace Center, Institute of Propulsion Technology, is employed to calculate the flow in the compressor.

1 Introduction

In order to increase safety and efficiency and decrease costs during the design and development process of modern aircraft, high efficient and accurate design tools are necessary. One demand on these tools is to predict the flow behavior on the aircraft fuselage and its wings as well as inside of the jet engine for an entire flight mission. To achieve this aim the flow physics have to be simulated correctly and therefore the interaction of the inner jet engine flow and the outer flow around the aircraft has to be taken into account. An accurate simulation is crucial for situations where high aerodynamic loads are present. Critical phases occur among others at take-off or flight through an area with strong crosswind, where highly turbulent air with both spacial and temporal varying flows may dominate the inflow of the jet engine. These intake distortions increase the risk of compression system instabilities and loss of efficiency. Inlet distortions may be composed of total pressure-, angle-, and total temperature distortions, depending on the particular configuration. All three disturbances cause a reduction of the stable operation range. Despite many experimental investigations, there is still a high demand for research in the field of inlet distortions. A good overview of the effects of intake distortion is given by Longley and Greitzer [1], as well as by Cousins [2]. Experimental investigations were carried out by Schmidt et al. [3], Peters et al. [4], [5], Reuss [6], Wadia et al. [7], [8]. In order to predict accurately the creation and the migration of the inlet disturbances and their

*Research scientist
†Research scientist
‡Professor

impact on the compressor, the aerodynamics in front of the engine and the flow into the jet engine have to be simulated simultaneously. At present, most of the numerical methods are specialized either for inner or for outer aerodynamics. One possibility to solve this problem is to couple two codes: one specialized for inner and the other for outer flow dynamics. This strategy is pursued by members of the DFG (German Research Foundation) research project FOR 1066, where two DLR codes TAU [9] and TRACE [10] are coupled. Validation tests of the TRACE-code are also presented with the focus on inlet distortion and its effect on compressor performance. These validation tests refer to a data set of a transonic compressor stage, which was experimentally investigated for homogenous [11] [12] and disturbed [13] inflow conditions at the DLR's Institute of Propulsion Technology in Cologne.

2 Description of the coupling tool

Most common flow solvers are specialized for some special area or technical application, such as compressible, incompressible flow, turbomachinery flow or outer aerodynamics. The majority are also able to solve problems that are not part of the original application but their performance suffers. In particular turbomachinery flow show features that are virtually unique. Examples are wake induced transition, circumferential periodicity and the influence of rotation. The general idea of coupling two codes is to fuse the strong points and to overcome the shortcomings of each code in different applications. The outer flow as flow around the airfoil, the nacelle, the fuselage and even meteorologic influences is calculated by one code and the inner flow through the engine is calculated by another code. Both are coupled by an interface. For the outer aerodynamics the DLR-TAU code and for the inner aerodynamics the DLR-TRACE code were chosen.

The TRACE code from the DLR Institute of Propulsion Technology is a well known and well validated code for the turbomachinery applications. The code allows the simulation of a multistage three-dimensional, periodically unsteady, and transitional flow on structured and hybrid grids. It solves the unsteady Reynolds averaged Navier-Stokes equations by means of a finite volume approach and it is optimized for the computation of turbomachinery internal flows. All convective fluxes are discretized using the TVD upwind scheme by Roe, which is combined with a MUSCL extrapolation scheme to gain second order accuracy in space. All diffusive fluxes are discretized using a second order central differencing scheme. For the steady state calculations presented in this paper, a time marching technique with an implicit predictor corrector scheme has been used. The dual time stepping approach used for the unsteady calculations utilizes an Euler implicit scheme within the pseudo-time level while a second order accurate Crank-Nicolson scheme is incorporated for physical time integration. The resulting linear system of equations is iteratively solved by a symmetric Gauss-Seidel relaxation scheme. For the inflow and outflow treatment non-reflecting boundary conditions are implemented. The CGNS (CFD General Notation System) file format is employed for the storage and retrieval of the flow field solution. More information about TRACE can be found in Yang et al. [12, 28], Nürnberger [29] and Eulitz [30].

The DLR-TAU code from the Institute of Aerodynamics and Flow Technology is a finite-volume flow solver for unstructured and hybrid meshes. To ensure low numerical diffusion all computations employ second-order central discretization with matrix-based artificial dissipation, while time integration is based on a second-order implicit dual-time stepping scheme. The flow field solution and the grid is stored by using the NetCDF (network Common Data Form) format. The DLR-Code is optimized and well validated for outer aerodynamics as flows around

airfoils and fuselage.

For all simulations presented in this study, turbulent flow is modelled using the Wilcox [26] k-w turbulence model.

The interface must be able to transfer the required information, be numerically stable and, for bigger calculations, be fast to maintain the computational performance. In this paper, a first version of an interface will be presented.

In figure 1, the concept of the coupling is shown for a simple channel flow. The upstream domain is calculated by TAU and the downstream domain is calculated by TRACE. In the version of the interface, presented here specified inlet and outlet boundary conditions are used. The interface transfers the primitive and the turbulent variables from TAU to TRACE, i.e. in flow direction, with only the static pressure communicated in the opposite direction. This is adequate as long as the convective flow crosses the interface only in one direction, which is from TAU domain to TRACE domain, in this case from upstream to downstream.

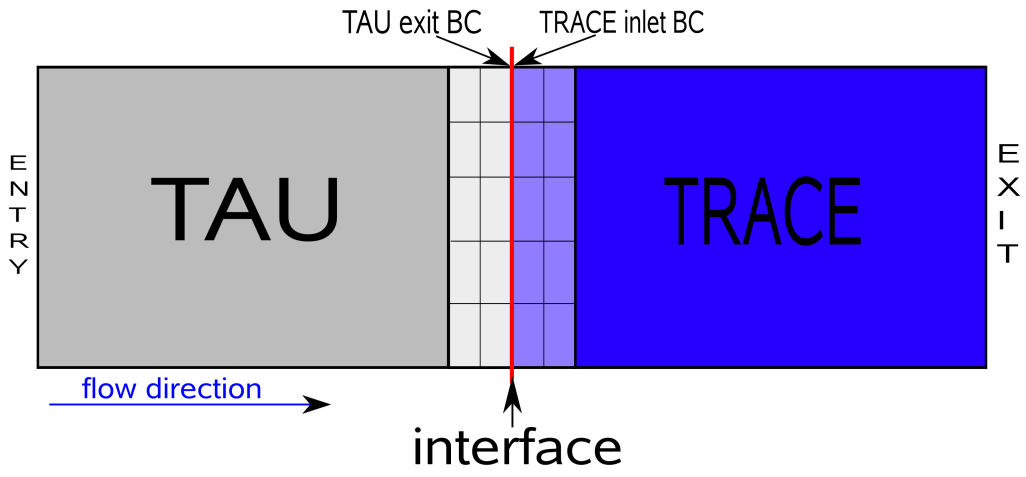

Figure 1: Concept of the code coupling

For validation, three test cases where used: a 2D flow over a flat plate, a 3D channel flow and a 3D flow in an annulus duct. The Mach number distribution for the annulus duct is shown, in figure 2. The boundary layer's gradient of growth is constant across the interface plane and the solution itself is physically reasonable. The other flow cases also show the same positive results.

The interface method also works for unsteady calculations. However, it has to be taken into account that it is not valid for implicit calculations, because the data transfer in this first version only occurs once every physical time step. The rate of communication between the two domains is too low for implicit calculations.

The coupling tool remains in development. Future version will incorporate the ability to model reverse flow as well as to improve the numerical performance.

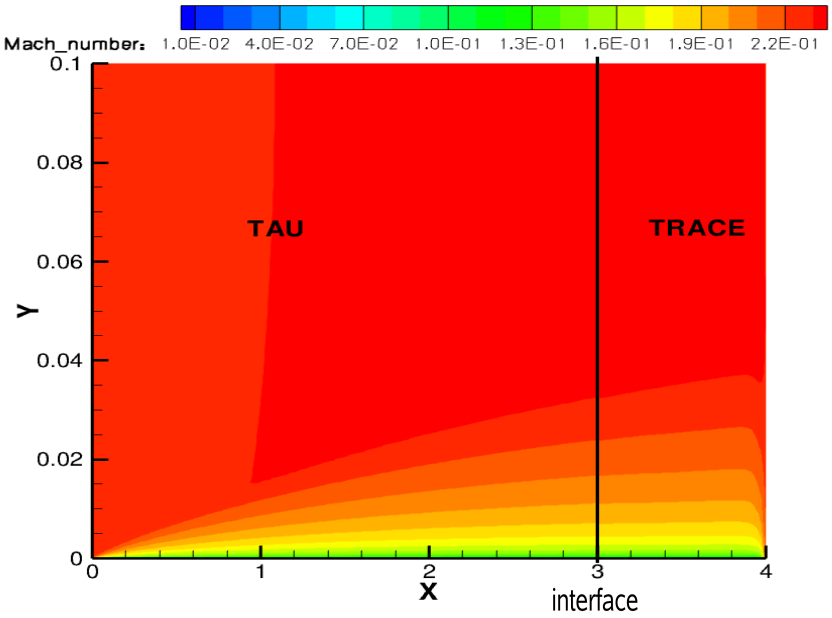

Figure 2: Mach number distribution in an annulus duct, coupled simulation with TAU and TRACE codes

3 Simulation of transonic compressor stage with distorted inflow

3.1 Description of the test case

The compressor stage shown in Fig. 3 was designed for a spool speed of 20260 RPM with a total pressure ratio of 1.51 at an equivalent mass flow of 17.3 kg/s under standard reference conditions (288 K and 101325 hPa). The rotor diameter is 398 mm with a hub-to-tip ratio of 0.5 and a maximum blade tip speed of 424 m/s. Overall, 28 blades with MCA profile and an average chord length of 50 mm were used.

Two different stator rows were used, depending on whether disturbed or undisturbed inflow conditions were applied: For homogeneous inflow conditions, the blade row consists of 60 blades with NACA-65-profiles, while for distorted inflow conditions 72 blades of the same profile were used. For the configuration with 28 rotor- and 60 stator blades, detailed temperature and pressure measurements as well as Laser2Focus measurements are available. For the second configuration, detailed measurements of temperature, pressure, and flow direction exist only for disturbed inflow conditions. In figure 3, the main parameters of the radial compressor are given. The inlet distortions were generated upstream of the compressor stage by a wake generator with non-rotating steel bars. The circumferential extent of these distortions was chosen as 60 and 120 degree. However, most of the published experimental data refer to a 120 degree-distortion.

3.2 Simulations

Four different types of numerical simulations were performed: Steady-state simulations for a one rotor and one stator blade passage, unsteady simulations for a configuration of one rotor blade passage and two stator blade passages [17] as well as steady and unsteady simulation for

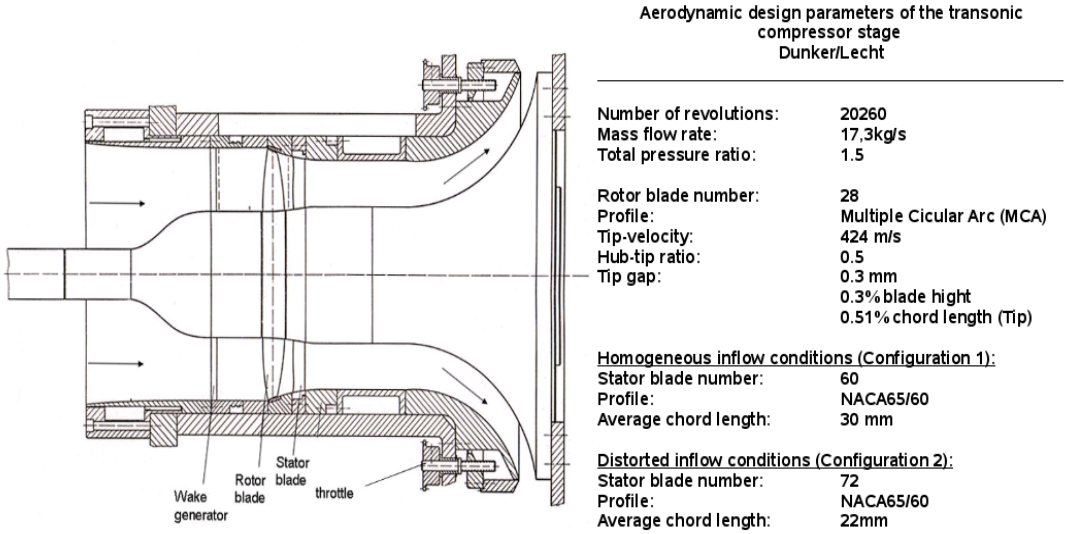

Figure 3: Transonic compressor stage and its aerodynamic parameters

the entire compressor stage. The first two simulation types were conducted with homogeneous inflow conditions. For steady runs, the mixing plane concept was applied. Here, identical flow conditions in all rotor and stator blade passages are assumed, meaning only one rotor and stator passage are required. The unsteady simulations were undertaken using the scaling technique, such that the number of rotor and stator blades must have a integer ratio. Thus, the stator geometry of configuration 1 had to be scaled down from 60 to 56 blades. Applying a grid with one rotor and two stator passages, results in a one-to-one match at the interface. The last two simulation types refer to distorted inflow conditions (configuration 2). Here no simplifications can be made and all 28 rotor and 72 stator passages have to be taken into account.

The simulations for homogeneous inflow conditions were conducted with a very high resolved computational grid in order to accurately simulate flow phenomena like the tip leakage flow, blade row interactions, and shock-boundary layer interaction. The boundary layers of the blade surfaces are resolved with more than 20 elements in the wall normal direction. Seven elements in the radial and 155 elements in the axial direction are used for the tip gap. The grid for the axial gap between the rotor trailing edge and the stator leading edge consists of 51 elements in axial direction, which permits an accurate simulation of the wake flow. For unsteady runs, the governing time dimension has to be highly discretised in order to predict accurately the transient nature of the tip leakage flow and wake flow. This time dimension is related to the blade passing frequency. Overall 512 physical time steps were used to resolve this passing frequency. A converged unsteady flow simulation of the blade passage was obtained after 8 blade passing periods. For flow-simulations with distorted inflow conditions, the high grid resolution was maintained. The computational grid consists of 766 structured blocks and more than 50 million grid points. The achieved maximum y+ values are lower than 1.5 where low Reynolds treatment were used (blades) and about 30 where wall functions were used (hub and tip walls).

3.3 Results of single passage simulations

In the first part of the investigation, steady and unsteady simulations were performed for homogeneous inflow conditions using the periodic boundary technique. The numerical investigations were conducted for the configuration of 28 rotor and 60 stator blades. This configuration was preferred, since the amount of experimental data for the second configuration with undisturbed inflow was limited. At the same time, a similar flow behaviour for both configurations can be assumed, as the same rotor geometry and the same stator profile was used.

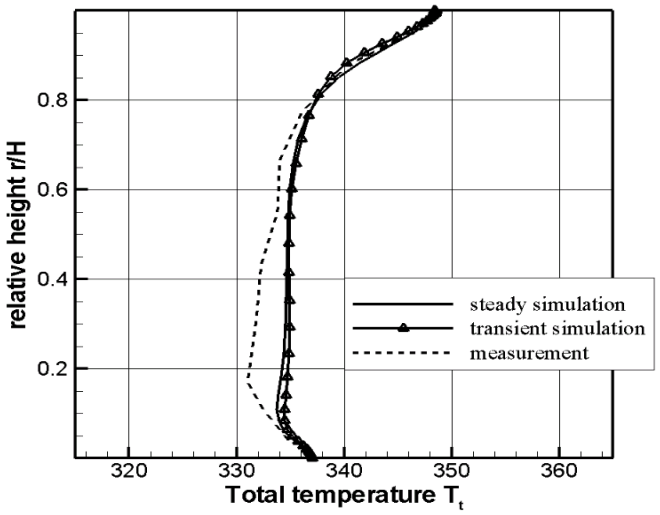

Figure 4: Measured and predicted temperature profiles at design conditions at stator exit near peak efficiency

Figures 4 and 5 display the radial profile of the total temperature at 100% rotational speed near peak efficiency and near stall downstream of the stator row. Steady as well as time-averaged unsteady numerical data are plotted. The temperature distributions show generally a good agreement, particularly between 80% and 100% span. The deviations generally do not exceed 1.5%. The differences between 20% and 80% are possibly due to the lack of a transition model. The temperature plots show that, steady and time-averaged unsteady numerical data are nearly the same. Obviously, the unsteadiness of the rotor stator interaction plays only a minor role at design speed.

The following two Figures display measured and simulated Mach number distributions at 100% rotational speed. Figure 6 show the Mach number distribution for design condition, figure 7 refer to flow conditions at high aerodynamic load. For both operating points, the time-averaged numerical data and the experimental data (acquired using the L2F-technique) show good agreement. The extent of the Prandtl-Meyer expansion, position and shape of the passage shock waves and Mach number levels for the whole rotor passage are well predicted. At design condition, both plots exhibit an oblique passage shock wave followed by a normal shock wave. Near instability onset, numerical and experimental data reveal a significant expansion on the suction side with Mach number values higher than 1.4. Furthermore, a detached normal shock has developed. Due to a significant shock-boundary layer interaction, a rapid growth

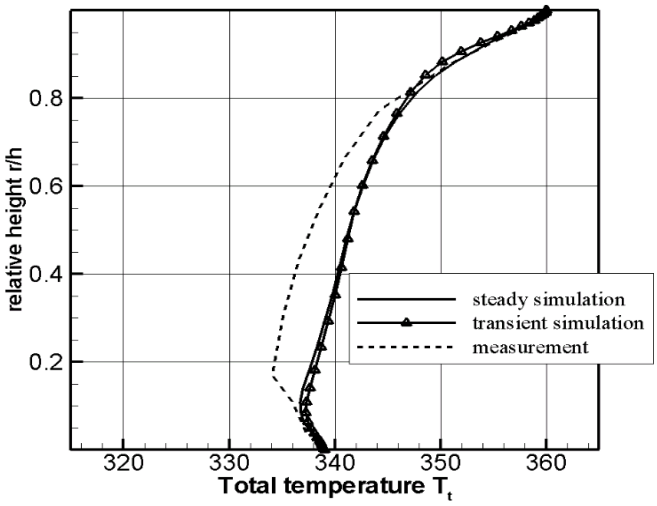

Figure 5: Measured and predicted temperature profiles at design conditions at stator exit near stall

of the boundary layer can be seen downstream of the shock position. Near the rotor tip, the boundary layer growth is underestimated by the simulation for high aerodynamic load. None the less, a good overall prediction of the flow behaviour in the rotor section is achieved.

With the experience gained in the first part of the project, further simulations were performed for the second compressor configuration with 72 instead of 60 stator blades. Since the geometry of the blades is identical, the stage geometry could be adjusted without great effort. Steady simulations for one blade passage and homogeneous inflow conditions were carried out as a first step. This was done in order to compare the predicted and measured performance offset caused by the disturbed inflow.

Figure 8 shows the compressor performance map for 85% rotational speed as calculated from numerical and experimental data. The plot contains performance values for several operating points between peak efficiency and instability onset. Efficiency and total pressure ratio are normalised with their respective values at peak efficiency. Overall, a similar behaviour with a decreasing mass flow rate can be found. As the performance data represent the only available experimental data without inlet distortions, a more detailed analysis cannot be performed.

3.4 Results of steady and unsteady simulations with distorted inlet

In order to accurately predict the boundary layer development and the behaviour of the tip leakage vortex, the high resolution of the grid was maintained from the single passage calculations, which leads to more than 50 million grid points. The simulations are carried out at 85% rotational speed near peak efficiency and near instability onset. The 85% characteristic is preferred, since more experimental data are available for this speed. Measured and simulated inflow conditions are plotted in figure 9. At midspan, the extent of the total pressure distortion is almost 120°degree and the pressure loss is up to 13%. Moreover, a small variation of the inflow angle can also be seen. The measured inflow conditions, which are used as the simulation

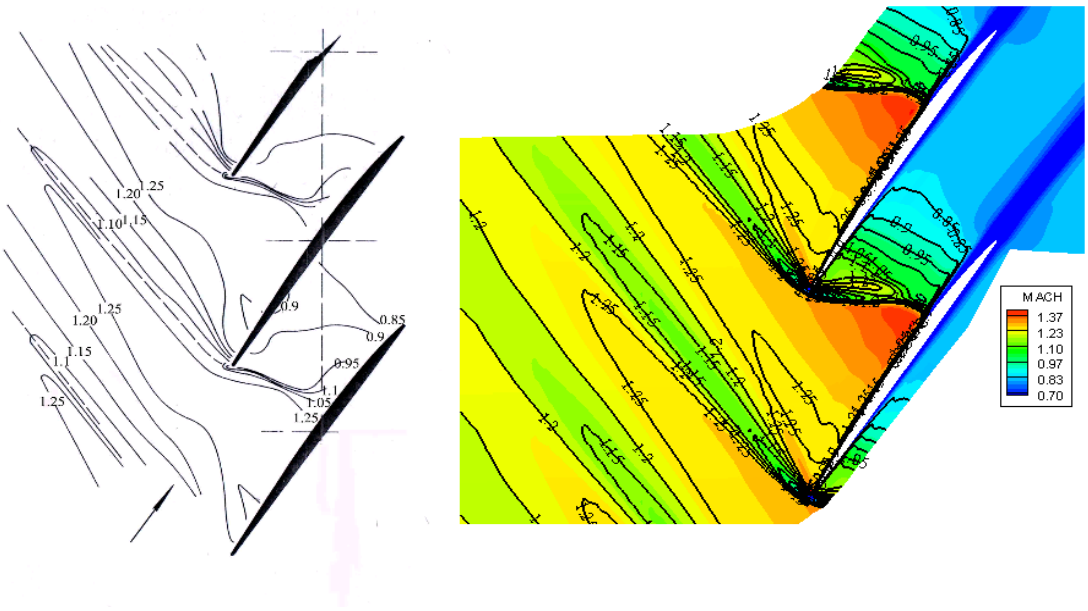

Figure 6: Measured (left) and simulated Mach number distribution at 69% span near stall and 100% rotational speed; numerical results are derived from time-averaged transient data

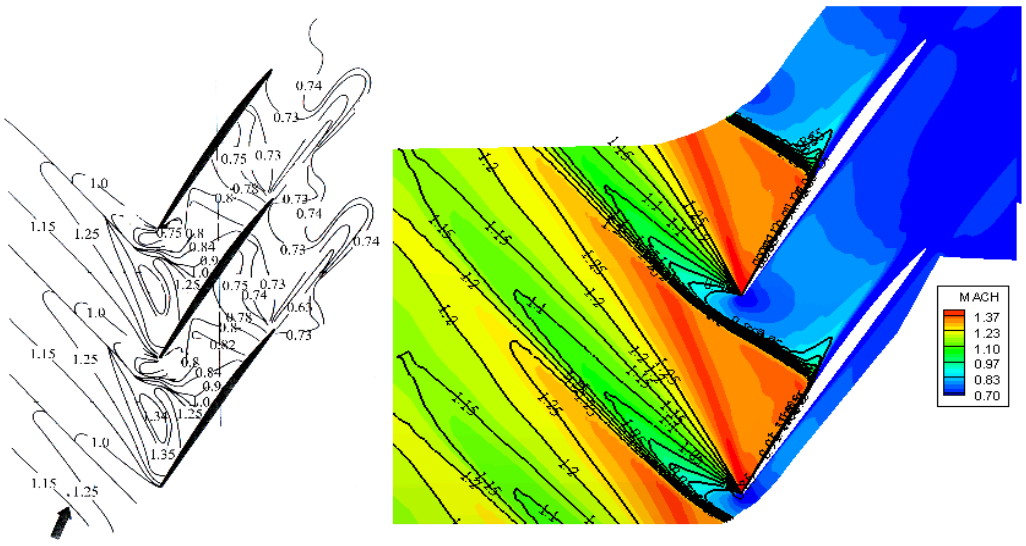

Figure 7: Measured (left) and simulated Mach number distribution at 69% span near stall and 100% rotational speed; numerical results are derived from time-averaged transient data

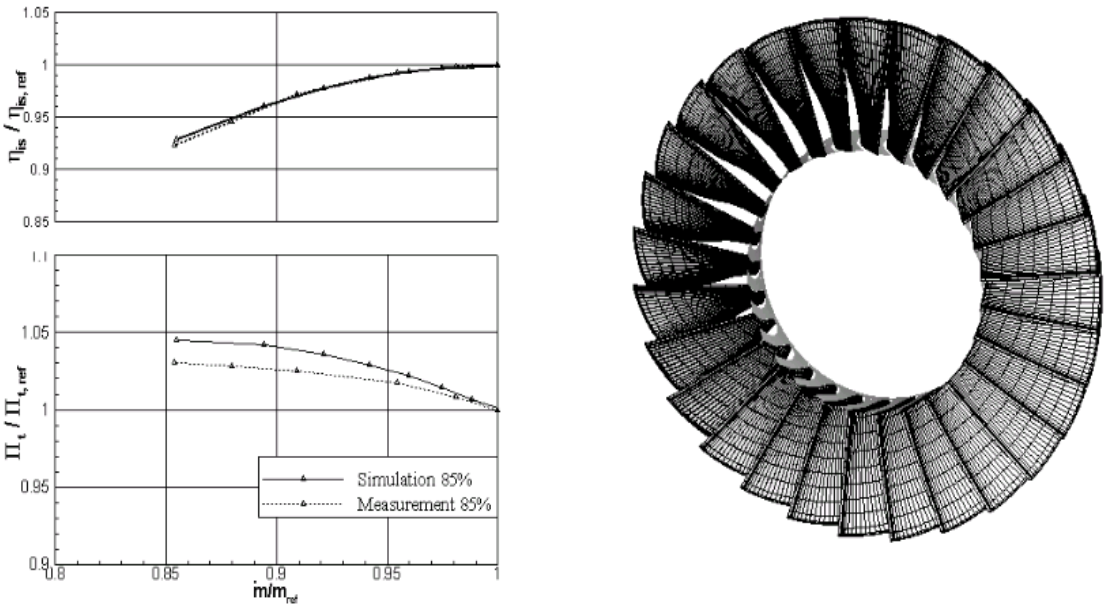

Figure 8: Performance map for the 85% characteristic, configuration of 28 rotor and 72 stator blades(left) and front view of the rotor blade row (right)

inlet boundary condition, are shown in Figure 9. The measurement plane, and consequently the simulation plane, is 50mm upstream of the compressore stage. The plot on the right hand side of Figure 9 shows the realization of the total pressure distortion at the inflow boundary. The total pressure as well as the inflow angle distribution were fixed by the inlet boundary condition. The simulation was carried out for about four rotor revolutions to assure a converged solution. In Figure 10, the time averaged Mach number distribution for two passages is shown. The picture on the left is for undistorted flow, while the one on the right is for a passage in the distorted region. The Mach number distribution for the passage with undistorted inflow shows no significant change to the blade passage simulations with homogeneous inflow conditions. The Mach number distribution for the other case show the influences of the distortion. Inside of the distortion, the smaller axial velocities lead to a higher incidence angle at the rotor leading edge. Hence, an increase of the aerodynamic load combined with an amplified normal shock occurs.

In Figure 11 the respective instantaneous entropy distributions are shown. The case on the left is for undistorted flow and on the right is for a distorted position. Entropy here is based on the undistored inflow conditions which means undistored total temperature and total pressure. One can see that the production of entropy is higher in the distorted zone. This can be explained by the fact that the blades are more highly loaded within the distorted area.

In Figure 12 the measured and the simulated total pressure distribution at mid span of the measuring plane after the stator row are shown. The trend of the total pressure distribution is well captured. The major difference is the stator wakes which can be seen in the simulation. The steady total pressure probes used and the coarse mesh of probe points are not able to

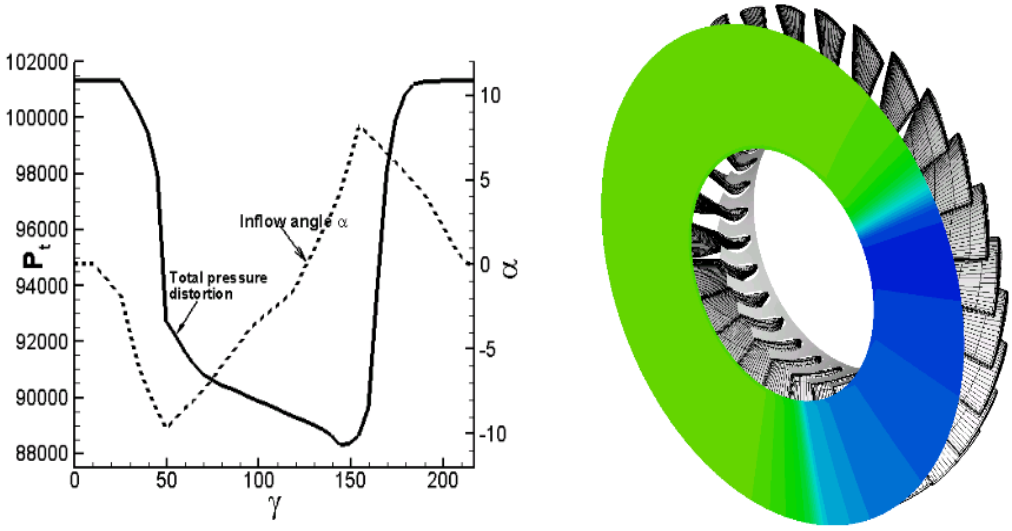

Figure 9: Measured and simulated inlet distortion at 85% rotational speed and the distorted flow.

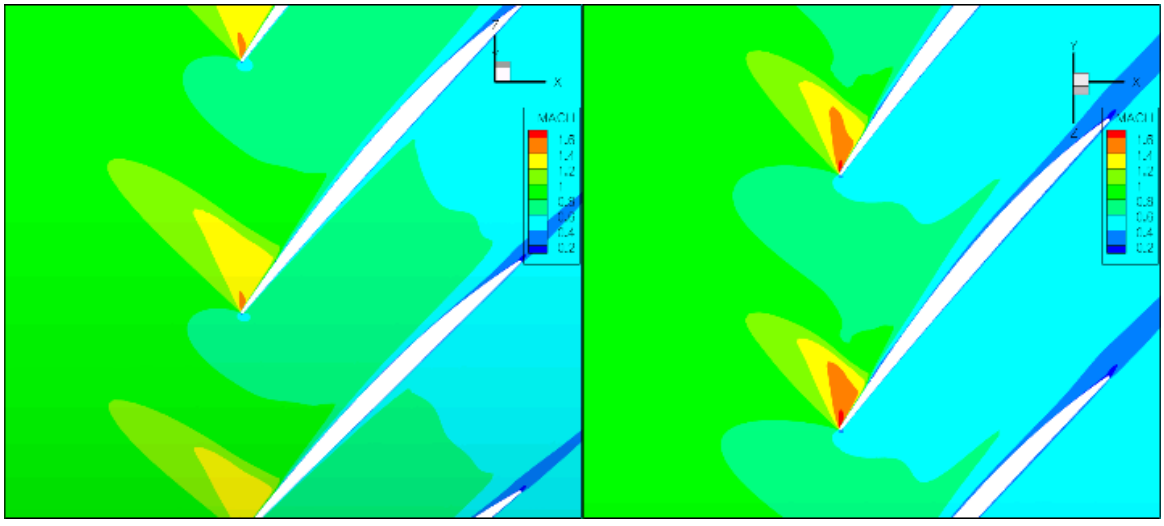

Figure 10: Mach number distribution at 85% rotational speed at design point; left undistorted inflow, right distorted inflow

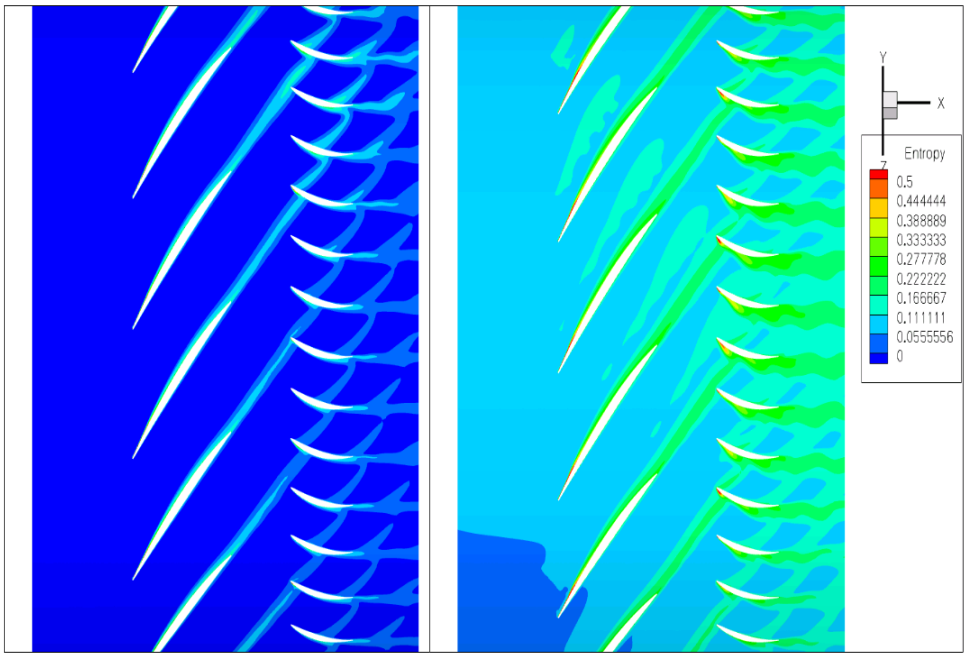

Figure 11: Entropy distribution at 85% rotational speed at design point; left undistorted inflow, right distorted inflow

resolve the stator wakes. Hence, there is no possibility to compare the simulated wake behavior and the measurements in more detail.

4 Conclusion and Outlook

Detailed numerical simulations were performed on a transonic compressor stage for homogeneous and disturbed inflow conditions. For homogeneous inflow conditions, a comparison between predicted and measured flow variables was conducted at different operating conditions. The comparison of circumferentially averaged total temperature profiles indicates that the differences are of an acceptable magnitude. The differences observed are possibly according to an inactivate transition model and therefore an underestimation of the secondary flow effects and profile losses. The simulated Mach number distributions at two different blade heights exhibit a good agreement with the experimental data from L2F-measurements. After checking the agreement between simulation and experiment for homogeneous inflow conditions, numerical simulations with total pressure distortions were carried out. Here, the assumption of periodicity between the blade passages is no longer valid. Thus, a full annulus calculation is required. The first results of the simulations have been presented, including a first comparison with measured data. The coupling tool which has been presented will also be further improved. A state-of-the-art compressor rig will be considered for further flow simulations with disturbed inflow conditions, where a rich experimental data set will be available for numerical validation.

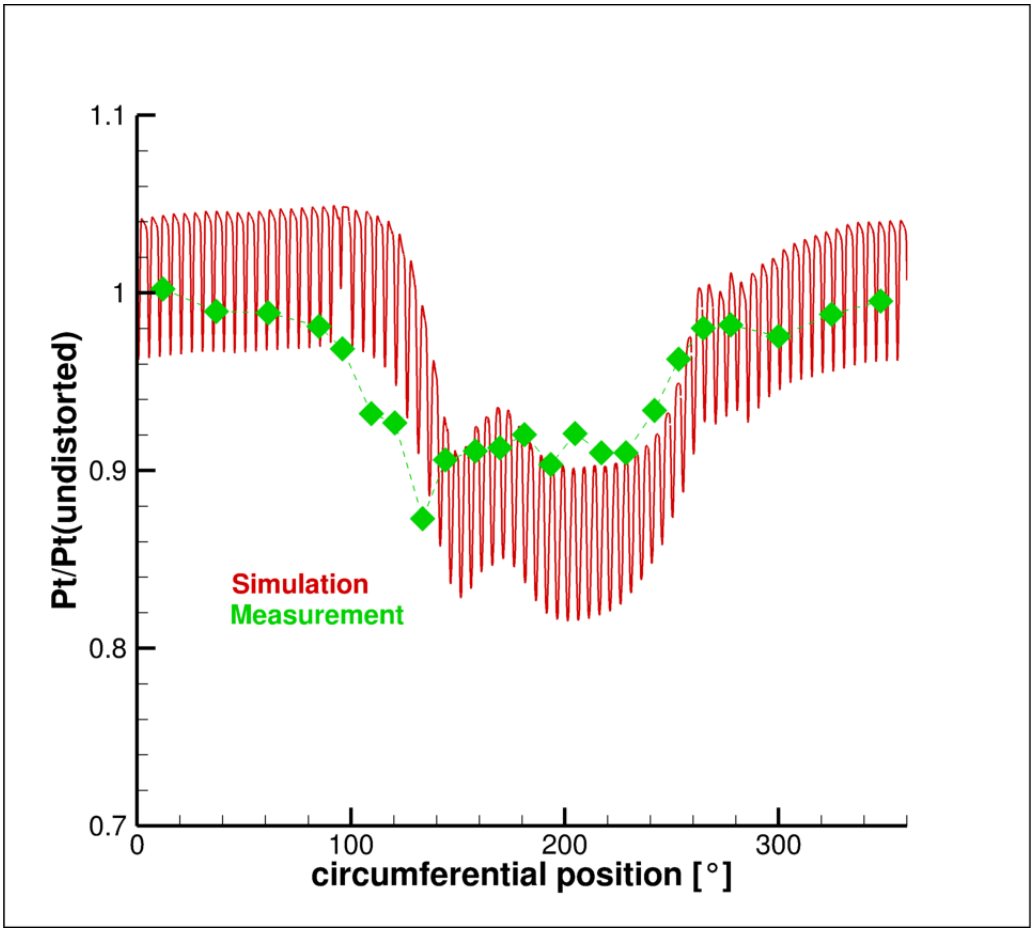

Figure 12: Outlet total pressure distribution at 85% rotational speed at design point

Acknowledgments

The members of the FOR 1066 research group gratefully acknowledge the support of the "Deutsche Forschungsgemeinschaft DFG" (German Research Foundation) which funded this research project.

References

[1] Longley, J.P. and Greitzer, E.M. 1992.: Inlet distortion effects in aircraft propulsion system integration. AGARD-LS-183

[2] Cousins, W.T. 2004.: History, philosophy, physics, and future directions of aircraft propulsion system inlet integration. ASME Paper GT2004-54210

[3] N.R., Leinhos, D.C., and Fottner, L. 2000.: Steady performance measurements of a turbofan engine with inlet distortions containing co- and counter-rotating swirl from an intake diffuser for hypersonic flight. ASME Paper 2000-GT-11

[4] Peters, T., Bürgener, T., and Fottner, L. 2001.: Effects of rotating inlet distortions on a 5-stage HP compressor. ASME Paper 2001-GT-0300

[5] Peters, T. and Fottner, L. 2002.: Effects of co- and counter-rotating inlet distortions on a 5-stage HP-compressor. ASME Paper 2002-GT-30395

[6] Reuss, N. 2005.: Untersuchung von kombinierten Eintrittstotaldruckstörungen auf das instationäre Betriebsverhalten eines fünfstufigen Hochdruckverdichters. Dissertation, Universität der Bundeswehr

[7] Wadia et al. 2002.: Forward swept rotor studies in multistage fans with inlet distortion. ASME Paper GT-2002-30326

[8] Wadia et al. 2008.: High-fidelity numerical analysis of per-rev-type inlet distortion transfer in multistage fans - Part I: simulations with selected blade rows. ASME Paper GT-2008-50812

[9] Klenner, J., Becker, K.; Cross, M., and Kroll, N. 2007.: Future simulation concept. 1st European CEAS Conference, Berlin

[10] Yang, H., Nürnberger, D., and Kersken, H.-P., 2006.: Toward excellence in turbomachinery computational fluid dynamics: A hybrid structured-unstructured reynolds-averaged navier-stokes solver. ASME Transactions, Journal of Turbomachinery, pp. 390-402, Vol. 128

[11] Dunker, R.J. and Hungenberg, H.G. 1980.: Transonic axial compressor using laser anemometry and unsteady pressure measurements. AIAA Journal, Vol 18, No. 8

[12] Dunker, R.J., Strinning, P., and Weyer, H.B. 1978. Experimental study of the flow field within a transonic axial compressor rotor by laser velocimetry and comparison with Through-Flow calculations, J. of Eng. For Power, Trans.ASME, Vol. 100, No. 2

[13] Lecht, M., 1983.: Beitrag zum Verhalten von Axialverdichterstufen bei stationärer Störung der Zuströmung. Forschungsbericht DFVLR Cologne

[14] Denton, J.D., 1990.: The calculation of three-dimensional viscous flows through multistage turbomachines, ASME Paper No. 90-GT-19, 1990

[15] Wilcox, D.C., 1998.: Turbulence modeling for CFD, 1998, Second Edition, DCW Industries, Anaheim

[16] Spalart, P. and Allmaras, S., 1992.: A one-equation turbulence model for aerodynamic flows, Technical Report AIAA-92-0439, 1992

[17] Iseler, J. and Niehuis, R. 2008.: Steady and unsteady flow-simulation of an axial transonic compressor stage, AIAA-2008-0083, 2008